Paleoelevation of Tibetan Lunpola basin in the Oligocene–Miocene transition estimated from leaf wax lipid dual isotopes

Guodong Jia [a,c,*], Yang Bai [a], Yongjia Ma [a], Jimin Sun [b], Ping'an Peng [a]

[a] State Key Laboratory of Organic Geochemistry, Guangzhou Institute of Geochemistry, Chinese Academy of Sciences, Guangzhou, China
[b] Institute of Geology and Geophysics, Chinese Academy of Sciences, Beijing, China
[c] Key Laboratory of Marginal Sea Geology, Guangzhou Institute of Geochemistry, Chinese Academy of Sciences, Guangzhou, China

A B S T R A C T

Carbon and hydrogen isotopic compositions of leaf wax *n*-alkanes are promising paleoelevation proxies. In this paper, the two proxies were applied to the Dingqing Formation in the Lunpola basin in the central Tibetan Plateau to reconstruct paleoelevation of the basin from the latest Oligocene to the early Miocene. Values of $\delta^{13}C$ and δD of C_{29} *n*-alkane were -29.8 ± 0.7 ‰ ($n = 38$) and -188 ± 10 ‰ ($n = 22$), respectively. Using the $\delta^{13}C$ and $\delta^{18}O$ of the early Miocene Siwalik paleosol carbonate in south Asia as lowland references, paleoelevation of ~3000 m was independently estimated from the two isotopic proxies. The results are consistent with recent estimates from pollen and mammal fossil studies. Furthermore, the time-series leaf wax $\delta^{13}C$ and δD records consistently suggest a reduction of ~900 m from 25.5 Ma to 21.6 Ma, which is likely associated with rapid erosion or tectonic unroofing.

© 2015 Elsevier B.V. All rights reserved.

1. Introduction

The surface uplift history of the Tibetan Plateau and Himalaya is increasing interests for its importance in reconstructing regional and global Cenozoic climate (Raymo and Ruddiman, 1992; Harris, 2006; Garzione, 2008) and in providing a robust test of the various models of continental deformation (Molnar et al., 2006; Rowley and Currie, 2006). Various methods have been applied to determine the paleoaltitude of the Tibetan Plateau, including the use of pollen assemblages (e.g., Song et al., 2010; Sun et al., 2014), fossil leaf physiognomy (Spicer et al., 2003), mammal fossils (Deng et al., 2012) and the oxygen isotopic composition of authigenic minerals (e.g., Garzione et al., 2000; Rowley and Currie, 2006). However, the plateau uplift history in space and time still remains for much debates.

In recent years, oxygen isotope paleoaltimetry, based on the systematic trends in the isotopic composition of modern precipitation of different topography, has been widely used in estimating paleoelevation in Tibet (e.g., Garzione et al., 2000; Cyr et al., 2005; Rowley and Currie, 2006; DeCelles et al., 2007; Xu et al., 2013). Reconstructed paleoelevation from $\delta^{18}O$ values of carbonates in the Cenozoic basins in Himalaya and Lhasa terranes demonstrates near-modern altitudes at least during the late Oligocene to middle Miocene (e.g., Rowley and Garzione, 2007; Quade

et al., 2011; Xu et al., 2013). These results not only largely predate the maximum elevation in the middle Miocene inferred from the ages of E–W extensional grabens in the Himalaya and Lhasa terranes (England and Houseman, 1988; Coleman and Hodges, 1995; Blisnuik et al., 2001), but also disagree with recently reported pollen and mammal fossil records arguing for a lower elevation during the late Oligocene and early Miocene (Deng et al., 2012; Sun et al., 2014). For example, Deng et al. (2012) discovered mammalian fossil of rhinocerotid, in the upper part of the Dingqing Formation in the Lunpola basin and inferred a paleoelevation close to 3000 m during the late Early Miocene. By using a refined chronology and high resolution palynological record of the uppermost Oligocene to the lower Miocene strata from the Lunpola Basin, Sun et al. (2014) indicated a maximum paleoelevation of 3190 ± 100 m during the period.

Each method for paleoelevation reconstruction has inherent strengths and weaknesses, and therefore, comparison of multi-proxy results is desired to avoid potential biases from single approach. Recently, a new approach to reconstructing paleoaltimetry using hydrogen isotope composition (δD) of plant leaf wax *n*-alkanes, reflective of δD of their growth water, was proposed and tested based on modern investigations along mountainous slopes surrounding or on the plateau (Jia et al., 2008; Luo et al., 2011; Bai et al., 2012) and applications to several ancient strata in the Lunpola basin and Hoh-Xil basin (Polissar et al., 2009). Further, carbon isotope composition ($\delta^{13}C$) of C_3 plant shifts positively with altitude globally as a result of decreasing temperature and atmospheric partial pressure of CO_2 and O_2 with altitude (Körner et al., 1988; 1991; Kelly and Woodward, 1995), and this trend has been documented and

exhibited in $\delta^{13}C$ values of surface soil organic matter and leaf wax n-alkanes along mountain slopes (Bird et al., 1994; Wei and Jia, 2009). These observations suggest that $\delta^{13}C$ of leaf wax n-alkanes may be an additional promising proxy for paleoelevation.

In the present work, the lower to middle Dingqing Formation in the Lunpola basin accumulated in the late Oligocene–early Miocene period was studied for paleoelevation using paired analysis of $\delta^{13}C$ and δD of sedimentary leaf wax n-alkanes. Previous studies yielded inconsistent paleoelevations in the same basin, with higher estimates from carbonate $\delta^{18}O$ method (Rowley and Currie, 2006) but lower values from pollen and mammal fossil studies (Deng et al., 2012; Sun et al., 2014). This paper aims to estimate paleoelevation of the Lunpola basin based on $\delta^{13}C$ and δD values of leaf wax n-alkanes, respectively.

2. Geological settings, samples and methods

The Lunpola basin is an east–west extended Tertiary sedimentary basin situated in the central Tibetan plateau with elevations varying between 4600 m and 5040 m above sea level (Fig. 1). The Cenozoic strata of the Lunpola basin are more than 4000 m thick, and consist of two primary stratigraphic units: the Niubao Formation in the lower part, and the Dingqing Formation in the upper part. In the present work, the studied section (32°04′19″N, 89°36′57″E, 4607 m asl), exposing the lower and middle Dingqing Formation (Fig. 2), is the same as that reported by Sun et al. (2014). The age of the section was determined to be from 25.5 to 19.8 Ma based on U–Pb zircon dating (He et al., 2012) and magnetostratigraphy correlations (Sun et al., 2014). A total of 38 bulk samples collected from the section, characterized by lacustrine fine-grained gray mudstone, were analyzed in this study (Fig. 3).

Samples of ~50 g were broken into 1–2 cm³ fragments, rinsed with dicloromethane (DCM) to remove any possible contamination from modern organic material, and then pulverized to fine powders. Powdered samples were ultrasonically extracted three times with DCM. The hydrocarbon fraction was isolated from the total extract using silica gel column chromatography (~2 g silica) by eluting with hexane (10 ml), and then purified for n-alkanes using urea adduction. Purified n-alkanes were then identified by comparison of retention times defined by gas-chromatography (GC) analysis of a mixed n-alkane

standards. The GC analysis was conducted using a Hewlett-Packard 6890 gas chromatograph with flame ionization detector (FID). The injector temperature was maintained at 290 °C, with a detector temperature of 300 °C. The GC oven program increased from 60°°C (held for 1 min) to 300 °C at 6 °C min⁻¹, and was held at 300 °C for 20 min.

Carbon isotopic analysis of n-alkanes was performed by gas chromatography–isotope ratio mass spectrometry (GC–IRMS), using an HP 6890 GC connected to a Delta Plus XL mass spectrometer via a GCC III interface. The temperature program and capillary column were identical to those used for GC analysis. Prior to analyses, the CO_2 reference gas was calibrated relative to VPDB. Instrument performance was routinely checked using GC–IRMS reference materials containing nine n-alkane homologues (C_{12}, C_{14}, C_{16}, C_{18}, C_{20}, C_{25}, C_{28}, C_{30}, and C_{32}). For isotopic standardization, CO_2 reference gas was automatically introduced into the mass spectrometer in a series of pulses at the beginning and the end of each analysis. Every sample was analyzed at least twice, and the average value, with $1\sigma \leq 0.6$ ‰, was reported here.

Hydrogen isotopic analyses of individual n-alkanes via gas chromatography–thermal conversion–isotope ratio mass spectrometry (GC–TC–IRMS) utilized an HP-6890 GC and a high-temperature pyrolysis unit that was connected on-line via a GCC III interface to a Finnigan MAT Delta Plus XL IRMS. Individual compounds separated by GC were pyrolysed to convert organic H into H_2 at 1450 °C, and the H_2 was then introduced into the mass spectrometer. The temperature program and capillary column were identical to those used for GC analysis. The H_3 factor for the mass spectrometer was determined every 6 injections using the standard hydrogen gas introduced through the interface, and its values were <5 ppm/nA during our sample analysis. The reproducibility and accuracy of the hydrogen isotopic analyses were evaluated routinely using the GC–IRMS reference n-alkane mixtures provided by Indiana University. Typically, during the analyses of unknown samples, laboratory standards were injected periodically (typically one standard injection per six sample analyses) to ensure that the mass spectrometer was stable. δD values of sample compounds were referenced to gaseous hydrogen which had been calibrated against the Indiana standard, independently calibrated against VSMOW-water. The standard deviations of duplicate analysis for n-alkanes ranged from 0 to 12 ‰.
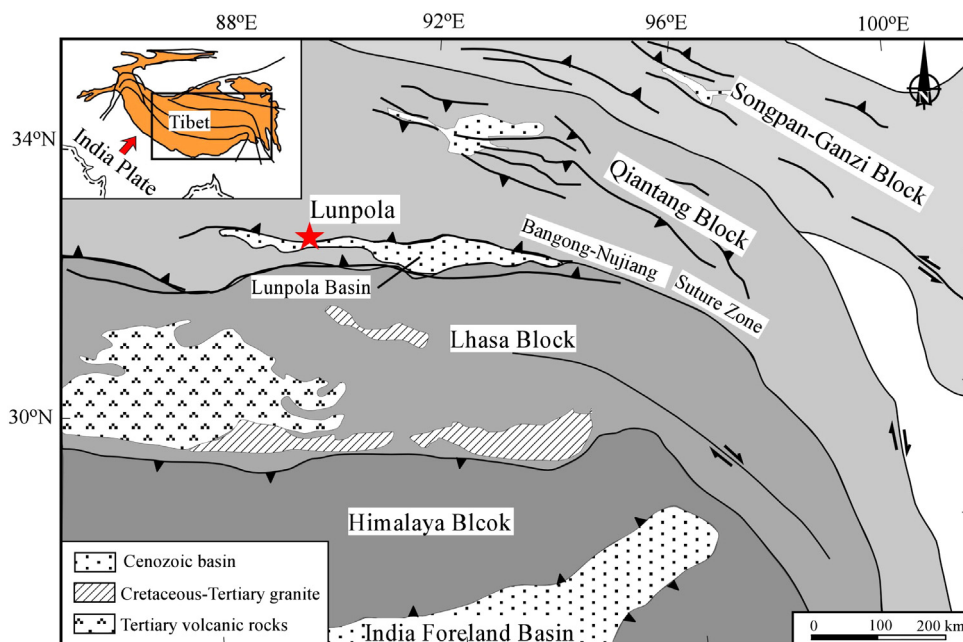

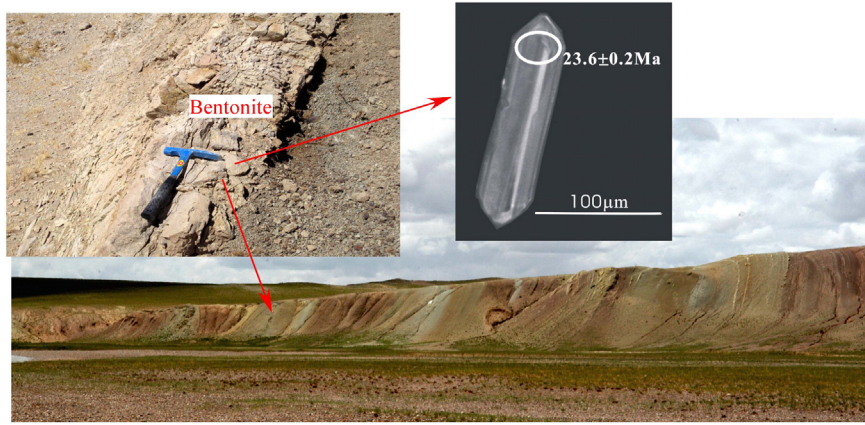Fig. 1. Simplified geologic map showing the tectonic framework of Tibet as well as the location of the Lunpola basin.

Fig. 2. Photos show the studied Dingqing Formation, the position of the Bentonite layer, and the U–Pb ages of zircons.

3. Results and discussion

3.1. n-alkane distribution and isotopic composition

The distribution of *n*-alkanes in all samples indicates minimal biological and diagenetic alterations. The *n*-alkanes contained a long-chain maxima (C_{29-33}) with a pronounced odd-over-even preference (OEP = 3.2 ± 0.9, n = 38) that is typical of epicuticular waxes from modern higher plants. A second maxima at shorter chain lengths (C_{16-18}) had almost no OEP and is attributable to algal and bacterial sources. All these characters are common for modern lake sediments

that receive organic material from both terrestrial plants and aquatic sources.

In our isotopic analysis, all the 38 samples yielded reliable *n*-alkane $\delta^{13}C$ values whereas only 22 of them yielded reliable δD values due to low amounts of *n*-alkanes. The $\delta^{13}C$ values of the odd carbon-numbered C_{27}, C_{29} and C_{31} *n*-alkanes were in similar ranges (-29.6 ± 0.6 ‰ for $\delta^{13}C_{27}$; -29.8 ± 0.7 ‰ for $\delta^{13}C_{29}$; -29.6 ± 0.6 ‰ for $\delta^{13}C_{31}$) and showed significant inter-correlations (e.g., $r^2 = 0.68$ between $\delta^{13}C_{27}$ and $\delta^{13}C_{29}$, $r^2 = 0.63$ between $\delta^{13}C_{29}$ and $\delta^{13}C_{31}$, $p < 0.001$) (Fig. 4a), demonstrating their similar carbon sources and photosynthetic pathways. Similarly, the δD values of C_{27}, C_{29} and C_{31}
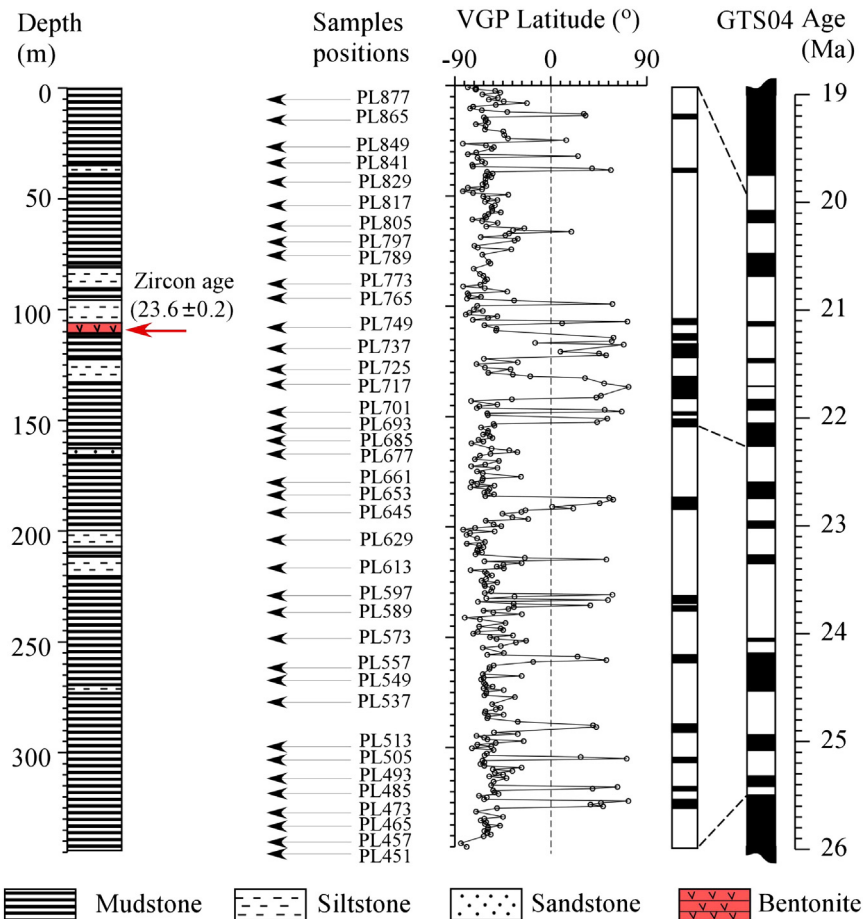

Fig. 3. The chronology of the Dingqing Formation (data after Sun et al., 2014) and the sampling positions of this study.
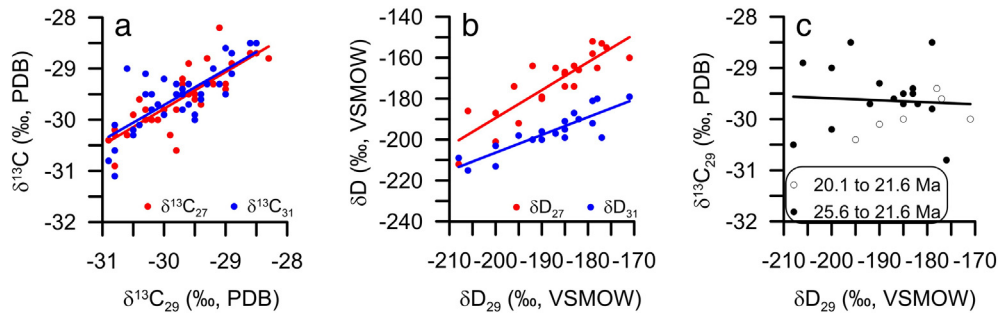
Fig. 4. Scatter plots of (a) $\delta^{13}C_{27}$ and $\delta^{13}C_{31}$ against $\delta^{13}C_{29}$, (b) δD_{27} and δD_{31} against δD_{29}, and (c) $\delta^{13}C_{29}$ against δD_{29}.

n-alkanes were also inter-correlated significantly (e.g., $r^2 = 0.79$ between δD_{27} and δD_{29}, $r^2 = 0.72$ between δD_{29} and δD_{31}, $p < 0.001$) (Fig. 4b). However, they showed values with distinct offsets, i.e., -172 ± 15 ‰, -188 ± 10 ‰, and -196 ± 11 ‰ for δD_{27}, δD_{29} and δD_{31}, respectively. The differences in δD values of leaf-wax lipids were also found in modern investigations but remain highly ambiguous for their causes, which are likely associated with their distinct water sources, fractionation processes or different groups of plants (Garcin et al., 2012).

In order to ascertain whether the original n-alkane δD signal was preserved during sedimentation, the δD of the isoprenoid compound phytane was measured in four samples in which phytane was in relatively high amounts, yielding a mean value of -315 ± 11 ‰. In contrast, δD values of the co-occurring C_{17} n-alkane was -146 ± 13 ‰. The

~170 ‰ more depleted value in phytane δD is comparable to those observed in modern plants and immature lacustrine sediments (e.g., Sessions et al., 1999; Chikaraishi and Naraoka, 2005; Pedentchouk et al., 2006), indicating preservation of the original n-alkane δD signal. Otherwise, thermal maturation would decrease the biosynthetic difference between isoprenoid and alkyl compounds to within 120 ‰ (Pedentchouk et al., 2006).

In this study, isotopic composition of C_{29} n-alkane was used to trace paleoenvironment, as conventionally done in the literature. No correlation can be observed between values of δD_{29} and $\delta^{13}C_{29}$ in a scatter plot (Fig. 4c). However, their time-series records exhibit clearly opposite trends from 25.5 to 21.6 Ma, i.e., a decreasing trend in $\delta^{13}C_{29}$ whereas an increasing trend in δD_{29}. After that until 20.4 Ma (below the top two samples), $\delta^{13}C_{29}$ and δD_{29} turned into increase and decrease,
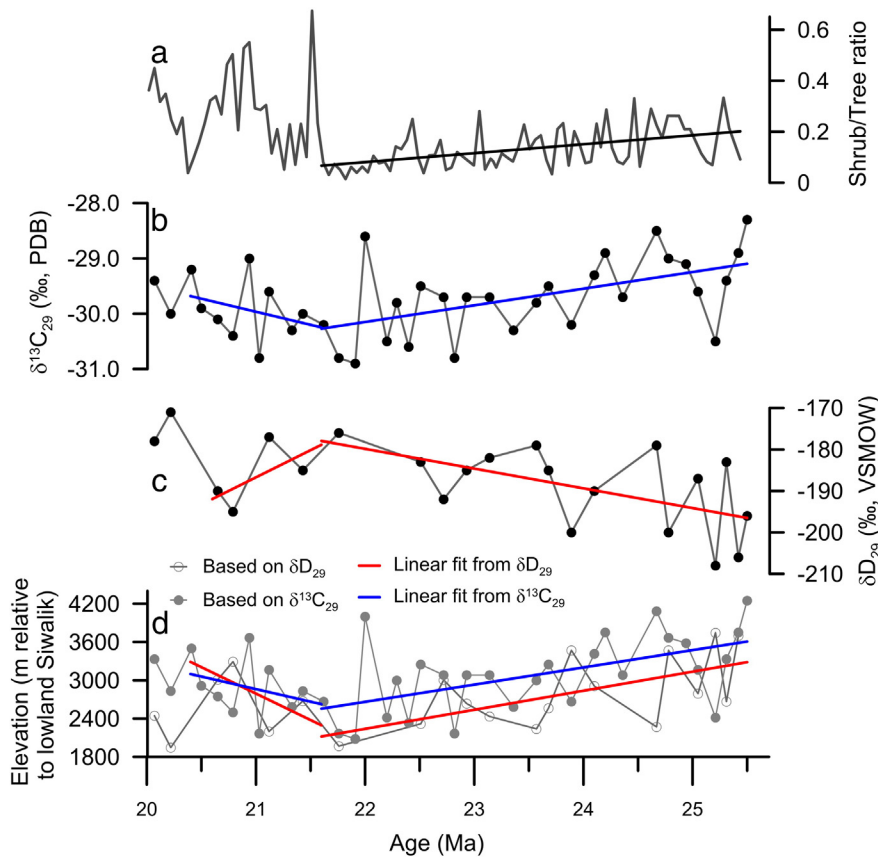
Fig. 5. Time-series records and estimated paleoelevation from Dingqing Formation. (a) The ratio of shrub to tree from pollen analysis (data from Sun et al., 2014); (b) $\delta^{13}C$ record of C_{29} n-alkane; (c) δD record of C_{29} n-alkane; and (d) estimated paleoelevation from $\delta^{13}C_{29}$ and δD_{29} values relative to the early Miocene lowland Siwalik deposit in South Asia. Straight lines are linear trends from 25.5 to 21.6 Ma and from 21.6 to 20.4 Ma, respectively. The top two sample data were not included in the linear regression.

respectively (Figs. 5b and c). The generally coordinate variation in δD_{29} and $\delta^{13}C_{29}$ implies that a common regulating factor controlled both δD_{29} and $\delta^{13}C_{29}$ in the long run. But the lack of correlation between δD_{29} and $\delta^{13}C_{29}$ values suggests that the deviations of the two isotopic ratios from their long-term trends are not associated with each other. This is likely due to environmental factors, such as temperature, humidity and vegetation, that at short terms may affect the δD_{29} and $\delta^{13}C_{29}$ values of leaf waxes in complex ways.

The long-term decrease of $\delta^{13}C_{29}$ from 25.5 to 21.6 Ma may reflect vegetation changes and suggest a wetting paleoclimate as indicated from pollen record showing a decrease of shrub-to-tree ratio in the same sedimentary section (Fig. 5a; Sun et al., 2014). After that, $\delta^{13}C_{29}$ increased correspondingly, although not proportionally, to the significant increase of shrub-to-tree ratio, suggesting a slightly drying period. Leaf wax δD is also affected by climate and vegetation, and usually displays lower values as results of greater isotopic fractionations by trees than by shrubs (e.g., Sachse et al., 2012) and lower δD of precipitation and soil water in wetter climates. The long-term increase of δD_{29} from 25.5 to 21.6 Ma, therefore, is apparently opposite to the decrease of shrub-to-tree ratio and wetting trend as indicated from pollen and $\delta^{13}C_{29}$ records. δD_{29} also varied in inverse direction to changes of vegetation and $\delta^{13}C_{29}$ after 21.6 Ma, when climate appeared to be slightly drying. This discrepancy implies that a common environmental factor beyond climate and vegetation regulated our observed long-term changes of leaf wax $\delta^{13}C$ and δD.

In this study, δD_{29} values are unlikely affected by evaporation, as commonly observed in arid climate, which may increase δD_{29} values under high evaporation by lowering the apparent isotopic fractionation between precipitation and leaf waxes (e.g., Polissar and Freeman, 2010). The observed inverse long-term change of δD_{29} to changes of vegetation and $\delta^{13}C_{29}$ also disapproves of evaporation as an influential factor. So δD_{29} is preferred as proxy of the isotopic composition of precipitation (δ_p). In low-latitude wet climate, δ_p is usually associated with local precipitation, i.e. the amount effect, with lighter δ_p values under high precipitation. However, this occurrence is not always the case. In fact, δ_p is determined by the degree of progressive removal of precipitation as it condenses from the water vapor during its transport, meaning that the cumulative precipitation amount in the whole transport pathways since the initial water vapor may be more important than the local one in regulating δp variations. And this scenario can be found along mountain slopes, where a concurrent decrease of both δ_p and local precipitation amount is a common phenomenon (Rowley and Garzione, 2007). Coincidentally, modern investigations show that an elevation transect provides conditions not only for δ_p decrease (e.g., Rowley and Garzione, 2007) but also for plant $\delta^{13}C$ increase (e.g., Körner et al., 1988, 1991) with the increase of elevation. We therefore hypothesize that the coupled opposite trends in our $\delta^{13}C_{29}$ and δD_{29} records are likely associated with elevation changes of the Lunpola basin catchments, as further discussed below.

3.2. Leaf wax $\delta^{13}C$ and paleoelevation (Fig. 6)

Plant $\delta^{13}C$ is acquired from isotope discrimination against atmospheric CO_2 ($\delta^{13}C_{atm}$) during photosynthesis. So values of $\delta^{13}C_{atm}$ in the past are required for accurate interpretation plant wax $\delta^{13}C$ records. According to Tipple et al. (2010), $\delta^{13}C_{atm}$ values during the latest Oligocene and early Miocene were ~ −6.0 ‰, therefore the apparent carbon isotopic fractionation factor for C_{29} n-alkane ($\varepsilon_{C_{29}-C_{O2}}$) in this study would be around −23.9 ± 0.7 ‰. This $\varepsilon_{C_{29}-CO_2}$ value is well within the range for C_3 plants between −33 and −19 ‰ compiled by Jia et al. (2012), which agrees with the pollen-inferred tree-dominated ecosystem for the time interval (Sun et al., 2014). However, the $\varepsilon_{C_{29}-CO_2}$ value of −23.9 ‰ is apparently positive relative to the $\varepsilon_{C_{29}-CO_2}$ mean values of −26.5 ‰ for C_3 plants.

The observed more positive $\varepsilon_{C_{29}-CO2}$ value, and hence more positive leaf wax $\delta^{13}C$, in the Lunpola basin is also evident when compared to
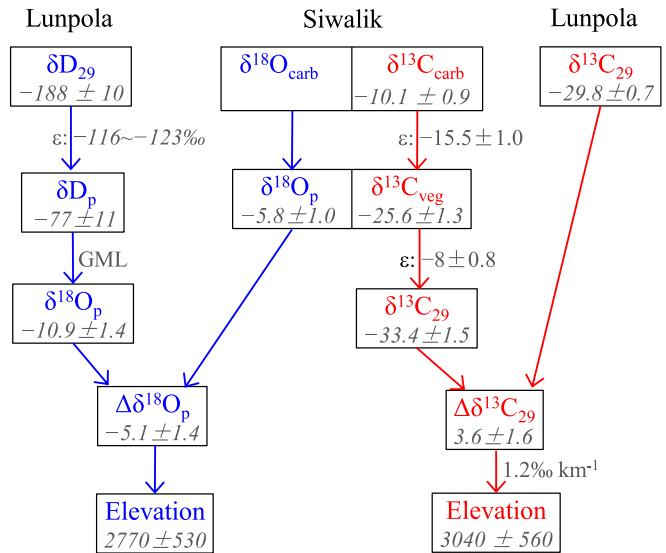

Fig. 6. Flow chart showing paleoelevation reconstruction using $\delta^{13}C$ and δD values of leaf wax C_{29} n-alkane in the Lunpola basin. The Siwalik basin is used as a low-elevation reference.

those inferred from the latest early Miocene pedogenic carbonate $\delta^{13}C$ from near-sea-level Siwalik foreland basin paleosols. The mean value of the pedogenic carbonate averaged −10.1 ± 0.9 ‰ ($n = 6$) during 17–15 Ma in the northern Pakistan (Quade and Cerling, 1995). Generally, soil carbonates are ~14 ‰ to 17 ‰ more ^{13}C-enriched relative to soil CO_2; the latter is primarily sourced from plant root respiration and microbial decomposition of soil organic matter, and its $\delta^{13}C$ value is nearly the same as that of aboveground vegetation (Amundson et al., 1998; Tipple and Pagani, 2007). So the paleovegetation $\delta^{13}C$ in the lowland Siwalik would be −25.6 ± 1.3 ‰ by assuming a mean enrichment value of 15.5 ± 1.0 ‰. This plant $\delta^{13}C$ value can be further converted to leaf wax $\delta^{13}C$ value with a fractionation factor, i.e., $\varepsilon_{C_{29}-bulk}$, which may depend on climatic regimes showing greater values in tropical areas and smaller ones in temperate areas (Vogts et al., 2009; Diefendorf et al., 2011). Pollen records in the Oligocene–Miocene South Asia have indicated a landscape comprising wet tropical evergreen forests in the lowlands, and moist deciduous forest with patches of pines at higher altitudes (Hoorn et al., 2000). Its modern analogs are likely the tropical rainforest in Africa and subtropical monsoon forest in China, where plants exhibit $\varepsilon_{C_{29}-bulk}$ values of −7.8 ± 2.2 ‰ ($n = 23$; Vogts et al., 2009) and −8.1 ± 1.5 ‰, respectively ($n = 4$; Bi et al., 2005). Paired $\delta^{13}C$ analysis of surface soil n-alkanes and bulk organic matter in forest ecosystems in Mount Gongga, eastern Tibetan Plateau, and East China show similar $\varepsilon_{C_{29}-bulk}$ values of −8.1 ± 1.3 ‰ ($n = 22$; Wei and Jia, 2009) and −8.1 ± 1.6 ‰ ($n = 31$; Rao et al., 2008). Here, the average of these reported $\varepsilon_{C_{29}-bulk}$ values, i.e., −8.0 ± 0.8 ‰, was used to convert plant $\delta^{13}C$ from the latest early Miocene Siwalik to C_{29} n-alkane $\delta^{13}C$, giving a value of −33.4 ± 1.5 ‰ that is close to the mean value for C_3 plants and more negative than the $\delta^{13}C_{29}$ value of −29.8 ± 0.7 ‰ from the Lunpola Basin.

Although the Siwalik samples were a bit younger than our latest Oligocene–early Miocene Lunpola samples, we surmise that they provided typical Neogene values of lowland South Asia before the rapid late Miocene expansion of C_4 plants (Tipple and Pagani, 2007). This surmise may be supported by the wet fluvial environment surrounded by tropical forests for the late Oligocene–early Miocene Chitarwata Formation that is similar to the middle Miocene Siwalik Formation in Pakistan (Hoorn et al., 2000; De Franceschi et al., 2008). The Chitarwata and Siwalik Formations are located at latitudes of ~30°N similar to the Lunpola basin at present. During the latest Oligocene–early Miocene period, their paleolatitudes were ~20°N due to the northward drift of

the Indian Plate (Métais et al., 2009), and pollen records have indicated mixed paleovegetation containing taxa from the tropical and subtropical rainforests, the temperate broadleaved forest and conifer forest, suggesting vertical zonal vegetation and thus the existence of neighboring elevated areas (De Franceschi et al., 2008; Sun et al., 2014). In spite of their similar paleolatitude and paleoenvironment, however, the $\delta^{13}C$ difference of C_{29} n-alkane between them, with a mean value of 3.6 ± 1.6 ‰ more positive in the Lunpola Basin, is remarkable.

Because $\delta^{13}C$ of C_3 plant is strongly negatively correlated with mean annual precipitation (MAP) (e.g., Diefendorf et al., 2010; Kohn, 2010), the difference in leaf wax $\delta^{13}C$ between the two areas might suggest a relatively humid paleoclimate in Pakistan and an arid one in the Lunpola basin. As an assumption, if the MAP was 2000–3000 mm yr^{-1} in Pakistan and the elevations was similar between the two areas, the 3.6 ± 1.6 ‰ positive shift in $\delta^{13}C$ in the Lunpola basin would indicate <500 mm MAP in the Lunpola Basin according to the equation for MAP as a function of $\delta^{13}C$ proposed by Kohn (2010). Thus low MAP, however, is not consistent with the pollen-indicated wet forest environment in the Lunpola basin (Sun et al., 2014). Alternatively, higher plant wax plant $\delta^{13}C$ values in the Lunpola basin may be associated with higher abundance of coniferous taxa (>30%; Sun et al., 2014), as evergreen gymnosperms isotopically less discriminate than other C_3 plants during photosynthesis (Diefendorf et al., 2010). However, the discrimination difference between them is 1–2 ‰ (Diefendorf et al., 2010; 2011), and thus even if coniferous abundance had been 100% in the Lunpola basin, it would not be adequate to account for the full range of the observed 3.6 ± 1.6 ‰ more positive $\delta^{13}C$.

Relatively higher abundance of coniferous taxa in the Lunpola basin was likely associated with its higher elevation during the Latest Oligocene and early Miocene; the latter might be the determinant of higher leaf wax $\delta^{13}C$ in the basin. And indeed, paleoelevation of the basin during the period has been inferred to be ~3000 m based on mammalian fossil (a rhinocerotid humerus, Deng et al., 2012) and pollen assemblages (Sun et al., 2014), or similar to present elevation of ~4600 m based on carbonate $\delta^{18}O$ (Rowley and Currie, 2006). In comparison, the latest Oligocene–middle Miocene foreland basin in South Asia was a near sea-level flood plain environment. Because C_3 plant $\delta^{13}C$ in humid area may shift positively with elevation, we believe that the paleoelevation difference between the two areas is responsible for the positive shift of vegetation $\delta^{13}C$ in the Lunpola Basin. Although the range of reported C_3 species-level response to elevation in humid areas is large (e.g., −0.9% to +2.7% km^{-1}; Körner et al., 1991), the average response to elevation based on thousands of C_3 plant species has been found to be 1.2 ± 0.9 ‰ km^{-1} with ranges from 1.1 to 1.3 ‰ km^{-1} from numerous mountain ranges of the globe (e.g., Körner et al., 1988, 1991; Li et al., 2007; Li et al., 2009). And moreover, this average species-level isotope response to elevation has been suggested to scale up linearly to community and landscape levels, which is ultimately and effectively documented by plant wax $\delta^{13}C$ at ~1.2 ‰ km^{-1} in the underlying mountain slope soils (Wei and Jia, 2009). By applying this elevational $\delta^{13}C$ gradient to the observed $\delta^{13}C$ differences between the Lunpola basin and the Siwalik Basin, a mean paleoelevation of ~3040 ± 560 m (1σ for 38 samples, not including uncertainties of each sample) for the Lunpola basin can be inferred (Table 1), which agrees to the previous estimates based on mammalian fossil and pollen analysis (Deng et al., 2012; Sun et al., 2014).

3.3. Leaf wax δD and paleoelevation (Fig. 6)

The δD value of plant-wax n-alkanes reflects that of precipitation, modified by soil evaporation, plant transpiration and biosynthesis. However, it is difficult to quantify each of these modifications on plant-wax δD, and current approaches use an apparent fractionation factor between precipitation and leaf waxes ($\varepsilon_{wax/p} = [(\delta D_{wax} + 1000) /$

$(\delta D_p + 1000)] - 1$, expressed in permil (‰)), which is an observed value that incorporates multiple, poorly understood fractionation steps. Although large scale surveys based on surface soils and lake sediments suggest that this $\varepsilon_{wax/p}$ is reasonably constant and thus δD_{wax} records variations in δD_p (Sachse et al., 2004; Hou et al., 2008; Feakins and Sessions, 2010; Sachse et al., 2012), plant-based surveys have revealed differences in $\varepsilon_{wax/p}$ among living plants when grouped according to plant functional type (PFT) (Liu et al., 2006; Smith and Freeman, 2006). Paleo-δD_{wax}, therefore, may be influenced by changes not only in δD_p, but also in vegetation, and thus values of $\varepsilon_{wax/p}$ have been vegetation-corrected before reconstructing paleo-δD_p in several recent studies (Collins et al., 2013; Feakins, 2013; Magill et al., 2013).

The recently reported pollen record in the same sedimentary section of this study (Sun et al., 2014) allow us to make fine corrections on $\varepsilon_{wax/p}$ in every sample based on pollen data in the same or adjacent sampling intervals, as have been performed by Feakins (2013). Pollen inferred PFTs in this study included trees, shrubs, C_3 herbs and ferns, whose mean values of $\varepsilon_{C_{29}/p}$ are −121 ± 22 ‰, −99 ± 32 ‰, −140 ± 31 ‰ and −108 ± 7 ‰, respectively, according to the compilation by Sachse et al. (2012) (in this study, C_3 herbs including forbs and C_3 grasses in the compilation). In the study section tree, shrub, herb and fern taxa occupied 70 ± 8%, 12 ± 7%, 11 ± 6% and 6 ± 2%, respectively, and did not vary greatly (Sun et al., 2014). We calculated the vegetation-corrected $\varepsilon_{C_{29}/p}$ ($\varepsilon_{vc-C_{29}/p}$) using the mean $\varepsilon_{C_{29}/p}$ values of each PFT and the relative PFT abundances estimated from pollen data, getting values of all our sample in a range between −123 ± 17 ‰ and −116 ± 16 ‰ (Table 1). This range of $\varepsilon_{vc-C_{29}/p}$ values is narrow because of the relatively stable vegetation pattern during the time interval and is similar to the value of −121 ± 10 ‰ suggested by Polissar and Freeman (2010) for the same formation in the Lunpola Basin. Using thus obtained $\varepsilon_{vc-C_{29}/p}$ values, δD_{29} values were then converted to δD_p, showing values of −62 ‰ to −99 ‰, with 1σ uncertainties between 14 ‰ and 20 ‰ contributed predominantly by those from $\varepsilon_{C_{29}/p}$.

In this study, paleoelevation was calculated from the difference between high- and low-elevation precipitation $\delta^{18}O$ ($\Delta\delta^{18}O_p$) using the model presented by Rowley (2007) (Fig. 6). This model is based on the premise of same moisture source for the high- and low-elevation sites, with the latter as a reference. For the Tibetan Plateau, this premise is particularly difficult to verify because the atmospheric circulation could have been changed by the development of the topography of Tibet and the Himalaya. In the southern plateau region, however, the Indian Ocean appears to remain the dominant source of moisture regardless of topography and plateau development based on global climate models (Saito et al., 2006). The Oligocene–Miocene paleolatitude of the Lunpola basin was ~20°N (Métais et al., 2009), considerably south of its present position and the current northern limit for Indian moisture (Tian et al., 2001). So, this configuration may suggest a common moisture source of Indian Ocean for the Lunpola and the Siwalik foreland basins. Therefore, the Siwalik foreland paleo-precipitation $\delta^{18}O$ was set as the low-elevation reference in this work, as has been done in previous studies (Rowley and Currie, 2006; Polissar et al., 2009; Quade et al., 2011; Gébelin et al., 2013). A $\delta^{18}O_p$ value of −5.8 ± 1.0 ‰ in the low-elevation foreland during the latest Oligocene–early Miocene has been estimated from both theoretical modeling (Quade et al., 2011) and Siwalik paleosol carbonate $\delta^{18}O$ (Gébelin et al., 2013). For the Lunpola basin, we recasted δD_{29}-derived δD_p values as $\delta^{18}O_p$ by means of the global meteoric water line, i.e., $\delta D = 8 \times \delta^{18}O + 10$. Then, the relative difference in $\delta^{18}O_p$ between the two locations was calculated and yielded a mean $\Delta\delta^{18}O_p$ value of −5.1 ‰ ranging from −7.8 ‰ to −3.2 ‰. Applying the model of Rowley (2007), this Miocene $\Delta\delta^{18}O_p$ between Lunpola and Siwalik corresponds to an elevation difference of ~2770 ± 530 m (1σ for 22 sample values, not including uncertainty in model estimates) (Table 1), which is also close to the previous estimates based on mammalian fossil and pollen records in the basin (Deng et al., 2012; Sun et al., 2014).

Table 1
$\delta^{13}C$ and δD values of leaf wax C_{29} n-alkane and estimated elevations.

Sample ID	Depth (M)	Age (Ma)	$\delta^{13}C_{29}$ (‰, PDB)	1σ SD	Elevation (m)[a]	δD_{29} (‰, VSMOW)	1σ SD	$\varepsilon_{C_{29}/p}$ (‰)	1σ SD	Elevation (m)	1σ SD[d]
PL877	5	20.1	−29.4	0.1	3333	−178	4	−115.5	17.1	2446	950
PL865	14	20.2	−30	0	2833	−171	−[b]	−116.2	15.5	1946	972
PL849	27	20.4	−29.2	0	3500	−[c]					
PL841	34	20.5	−29.9	0	2917	−[c]					
PL829	43	20.7	−30.1	0.3	2750	−190	4	−117.7	14.2	3012	687
PL817	53	20.8	−30.4	0.4	2500	−195	4	−117.5	15.5	3294	681
PL805	62	20.9	−29	0.3	3667	−[c]					
PL797	69	21.0	−30.8	0.1	2167	−[c]					
PL789	75	21.1	−29.6	0.2	3167	−177	4	−118.4	16	2199	950
PL773	89	21.3	−30.3	0	2583	−[c]					
PL765	95	21.4	−30	0.5	2833	−185	2	−118.9	16.6	2676	850
PL749	108	21.6	−30.2	0	2667	−[c]					
PL737	117	21.8	−30.8	0.4	2167	−176	2	−121.3	17.8	1969	1082
PL725	127	21.9	−30.9	0	2083	−[c]					
PL717	133	22.0	−28.6	0.2	4000	−[c]					
PL701	146	22.2	−30.5	0	2417	−[c]					
PL693	153	22.3	−29.8	0.5	3000	−[c]					
PL685	159	22.4	−30.6	0.6	2333	−[c]					
PL677	165	22.5	−29.5	0.1	3250	−183	−[b]	−122.6	16.6	2319	954
PL661	178	22.7	−29.7	0.4	3083	−192	−[b]	−120.3	17.3	3006	826
PL653	184	22.8	−30.8	0.6	2167	−[c]					
PL645	191	22.9	−29.7	0.3	3083	−185	0	−119.7	19.7	2637	1004
PL629	204	23.1	−29.7	0.2	3083	−182	0	−119.8	17.2	2434	928
PL613	216	23.4	−30.3	0.3	2583	−[c]					
PL597	229	23.6	−29.8	0.1	3000	−179	2	−120	16.7	2239	956
PL589	236	23.7	−29.5	0.6	3250	−185	1	−121.3	17.5	2564	916
PL573	248	23.9	−30.2	0.1	2667	−200	3	−119.3	17.3	3469	701
PL557	261	24.1	−29.3	0.1	3417	−190	0	−120	17.7	2911	839
PL549	267	24.2	−28.9	0.2	3750	−[c]					
PL537	276	24.4	−29.7	0.5	3083	−[c]					
PL513	295	24.7	−28.5	0.3	4083	−179	−[b]	−119.5	15.1	2270	878
PL505	302	24.8	−29	0	3667	−200	6	−119.1	16.3	3469	698
PL493	311	24.9	−29.1	0	3583	−[c]					
PL485	318	25.1	−29.6	0	3167	−187	12	−119	16.7	2793	1024
PL473	327	25.2	−30.5	0.2	2417	−208	1	−120.7	18.4	3745	664
PL465	334	25.3	−29.4	0.4	3333	−183	2	−117	16	2667	823
PL457	340	25.4	−28.9	0.1	3750	−206	−[b]	−120.2	16.1	3698	611
PL451	345	25.5	−28.3	0.4	4250	−196	7	−121.8	17.4	3136	839

[a] Elevation was estimated using a $\delta^{13}C$ gradient of 1.2 ‰ km^{-1}. The uncertainties are difficult to estimate, but may come mainly from the conversion of lowland Siwalik carbonate $\delta^{13}C$ to $\delta^{13}C_{29}$ with uncertainty of ~1.5 ‰ (see text), corresponding to ~1250 m.

[b] No 1σ estimates because of only one analysis due to low amounts of n-alkanes.

[c] No reliable data obtained because of low amounts of n-alkanes.

[d] Estimated using the error propagation equation and 1σ uncertainties of δD_{29}, $\varepsilon_{C_{29}/p}$, and early Miocene lowland Siwalik $\delta^{18}O$. Overall uncertainties were contributed predominantly from $\varepsilon_{C_{29}/p}$.

3.4. Elevation changes from the latest Oligocene to early Miocene

Previous studies using carbonate $\delta^{18}O$ and plant wax δD from the Miocene Dingqing Formation in the Lunpola basin showed paleoelevations in excess of 4000 m (Rowley and Currie, 2006; Polissar et al., 2009), apparently higher than our estimates here. Our new mean paleoelevation reconstructed independently from plant wax $\delta^{13}C$ and δD, as well as their agreement with mammalian fossil and pollen records in the same basin, convinces us of the reliability of the reconstructions in this study. The cause of the different paleoelevation results is unclear at present, but we surmise that it might be associated with a different type of samples in these studies. Lacustrine and palaeosol carbonates were analyzed in the works of Rowley and Currie (2006) and Polissar et al. (2009). Carbonate diagenetic alteration at high-temperature and/or by ^{18}O-depleted waters may result in a reduction in $\delta^{18}O$ compositions that may lead to erroneous interpretations of palaeoelevation (Garzione et al., 2004). Resetting of $\delta^{18}O$ values in carbonate has been found to begin at burial temperature >100–120 °C (Mora et al., 1998; Leier et al., 2009), which likely has occurred in the Lunpola basin given the enormously high thermal gradient of 50–70 °C km^{-1} (Yuan and Xu, 2000; Liu et al., 2001) and >4 km thick strata. Besides, diagenetic carbonate dissolution and cementation by younger meteoric waters, likely ^{18}O-depleted and contaminated by D-depleted younger plant wax lipids, in the basin strata have been

recognized (Ai et al., 1999). Nevertheless, further works are needed to clarify this issue.

The coupled time-series trends of $\delta^{13}C$ decrease and δD increase during the latest Oligocene and early Miocene (Figs. 5b and c) may provide further critical information of changes in the mean elevation of the basin catchments, because both of the records suggest the same trend of elevation changes during the time period (Fig. 5d). A similar average of 900 m reduction in paleoelevation from 25.5 to 21.6 Ma and then 500 or 1000 m rise from 21.6 to 20.4 Ma could be estimated based on the linear trends of $\delta^{13}C_{29}$ and δD_{29} records, respectively. The difference in elevation rise from 21.6 to 20.4 Ma from the two proxies may be due to the quite few data of δD_{29} for the linear regression. The inferred reduction of elevation from 25.5 to 21.6 Ma was consistent with the warming and wetting trend, favoring intensive erosion, indicated by pollen record during the time period (Sun et al., 2014), although climate change might be an alternative cause for the latter.

The inferred elevation reduction from 25.5 to 21.6 Ma does not support the point that once elevated since the Eocene the plateau's mean elevation did not vary (Rowley and Currie, 2006), although our results cannot tell whether erosion by climate weathering (Harris, 2006) or tectonic unroofing associated with, e.g., east–west extension (Molnar et al., 2006), was responsible for the elevation reduction. At least, intensive erosion has been evidenced by several investigations. For example,

the well preserved and widely distributed peak planation surface on the plateau, suggestive of extensive weathering and high erosion, was formed during the Oligocene and early Miocene, and especially during 30–20 Ma in central Tibet (Ding et al., 2000). Rapid erosion was also suggested from the brief period of extremely rapid mineral cooling at sometimes in the interval of 26–15 Ma inferred from thermochronometric data from plutons in south-central Tibet (Copeland et al., 1995). Subsidence analysis of the Lunpola basin exhibited a persistent subsiding history from the Eocene to the early Miocene (Ma et al., 2013), also supportive of our inference.

4. Conclusions

Modern observations show that carbon and hydrogen isotopic compositions of higher plants vary systematically with elevations, thereby making them feasible to trace paleoelevation from sediment records. In this study, carbon and hydrogen isotopic compositions of leaf wax *n*-alkanes were combined to reconstruct the paleoelevation of the Lunpola basin during the latest Oligocene–early Miocene when the Dingqing Formation accumulated. Dual isotope application allowed a cross check of the independently estimated paleoelevations. The similar estimates, i.e., 3040 ± 560 ($n = 38$) from $\delta^{13}C$ and 2770 ± 530 ($n = 22$) from δD, as well as their accordance with those from pollen and mammal fossil studies, corroborated the reliability of the dual isotope methods. Moreover, both the time-series $\delta^{13}C$ and δD records suggested a reduction of ~900 during 25.5 and 21.6 Ma and then a rise of several hundred meters thereafter. The inferred variation in elevation was not reported previously and remains to be validated in future studies.

Acknowledgment

References

Ai, H.G., Zhu, H.Q., Zhang, K.Y., Zeng, T., Luo, Y., 1999. The diagenetic controlling-factors of reservoir property and diageneses of reservoir of lower-Tertiary in Lunpola Basin, Tibet. Acta Sedimentol. Sin. 17 (1), 100–105 (In Chinese with English abstract).

Amundson, R., Stern, L., Baisden, T., Wang, Y., 1998. The isotopic composition of soil and soil-respired CO_2. Geoderma 82, 83–114.

Bai, Y., Fang, X., Tian, Q., 2012. Spatial patterns of soil *n*-alkane δD values on the Tibetan Plateau: implications for monsoon boundaries and paleoelevation reconstructions. J. Geophys. Res. 117. http://dx.doi.org/10.1029/2012JD017803 D20113.

Bi, X., Sheng, G., Liu, X., Li, C., Fu, J., 2005. Molecular and carbon and hydrogen isotopic composition of *n*-alkanes in plant leaf waxes. Org. Geochem. 36, 1405–1417.

Bird, M.I., Haberle, S.G., Chivas, A.R., 1994. Effect of altitude on the carbon-isotope composition of forest and grassland soils from Papua New Guinea. Global Biogeochem. Cycles 8, 13–22.

Blisnuik, P.M., Hacker, B.R., Glodny, J., Ratschbacher, L., Bi, S., Wu, Z., McWilliams, M.O., Calvert, A., 2001. Extension in central Tibet since at least 13.5 Myr. Nature 412, 628–632.

Chikaraishi, Y., Naraoka, H., 2005. $\delta^{13}C$ and δD identification of sources of lipid biomarkers in sediments of Lake Haruna (Japan). Geochim. Cosmochim. Acta 69, 3285–3297.

Coleman, M., Hodges, K., 1995. Evidence for Tibetan Plateau uplift before 14-Myr ago from a new minimum age for east–west extension. Nature 374, 49–52.

Collins, J.A., Schefuß, E., Mulitza, S., Prange, M., Werner, M., Tharammal, T., Paul, A., Wefer, G., 2013. Estimating the hydrogen isotopic composition of past precipitation using leaf-waxes from western Africa. Quat. Sci. Rev. 65, 88–101.

Copeland, P., Harrison, T.M., Pan, Y., Kidd, W.S.E., Roden, M., Zhang, Y., 1995. Thermal evolution of the Gangdese batholith, southern Tibet: a history of episodic unroofing. Tectonics 14, 223–236.

Cyr, A., Currie, B.S., Rowley, D.B., 2005. Geochemical and stable isotopic evaluation of Fenghuoshan Group lacustrine carbonates, north-central Tibet: implications for the paleoaltimetry of late Eocene Tibetan Plateau. J. Geol. 113, 517–533.

De Franceschi, D., Hoorn, C., Antoine, P.-O., Cheema, I.U., Flynn, L.J., Lindsay, E.H., Marivaux, L., Métais, G., Rajpar, A.R., Welcomme, J.-L., 2008. Floral data from the mid-Cenozoic of central Pakistan. Rev. Palaeobot. Palynol. 150, 115–129.

DeCelles, P.G., Quade, J., Kapp, P., Fan, M.J., Dettman, D.L., Ding, L., 2007. High and dry in central Tibet during the Late Oligocene. Earth Planet. Sci. Lett. 253, 389–401.

Deng, T., Wang, S.Q., Xie, G.P., Li, Q., Hou, S.K., Sun, B.Y., 2012. A mammalian fossil from the Dingqing Formation in the Lunpola Basin, northern Tibet, and its relevance to age and paleo-altimetry. Chin. Sci. Bull. 57, 261–269.

Diefendorf, A.F., Mueller, K.E., Wing, S.L., Koch, P.L., Freeman, K.H., 2010. Global patterns in leaf ^{13}C discrimination and implications for studies of past and future climate. Proc. Natl. Acad. Sci. U. S. A. 107, 5738–5743.

Diefendorf, A.F., Freeman, K.H., Wing, S.L., Graham, H.V., 2011. Production of *n*-alkyl lipids in living plants and implications for the geologic past. Geochim. Cosmochim. Acta 75, 7472–7485.

Ding, L., Zhou, Y., Zhang, J.J., Deng, W.M., 2000. Geologic relationships and geochronology of the Cenozoic volcanoes and interbedded weathered mantles of Yulinshan in Qiangtang, North Tibet. Chin. Sci. Bull. 45, 2214–2220.

England, P.C., Houseman, G.A., 1988. The mechanics of the Tibetan Plateau. Philos. Trans. R. Soc. Lond. A 26, 301–320.

Feakins, S.J., 2013. Pollen-corrected leaf wax D/H reconstructions of northeast African hydrological changes during the late Miocene. Palaeogeogr. Palaeoclimatol. Palaeoecol. 374, 62–71.

Feakins, S.J., Sessions, A.L., 2010. Controls on the D/H ratios of plant leaf waxes in an arid ecosystem. Geochim. Cosmochim. Acta 74, 2128–2141.

Garcin, Y., Schwab, V.F., Gleixner, G., Kahmen, A., Todou, G., Séné, O., Onana, J.-M., Achoundong, G., Sachse, D., 2012. Hydrogen isotope ratios of lacustrine sedimentary *n*-alkanes as proxies of tropical African hydrology: insights from a calibration transect across Cameroon. Geochim. Cosmochim. Acta 79, 106–126.

Garzione, C.N., 2008. Surface uplift of Tibet and Cenozoic global cooling. Geology 36, 1003–1004.

Garzione, C.N., Dettman, D.L., Quade, J., DeCelles, P.G., Butler, R.F., 2000. High times on the Tibetan plateau: paleoelevation of the Thakkhola graben, Nepal. Geology 28, 339–342.

Garzione, C.N., Dettman, D.L., Horton, B.K., 2004. Carbonate oxygen isotope paleoaltimetry: evaluating the effect of diagenesis on paleoelevation estimates for the Tibetan plateau. Palaeogeogr. Palaeoclimatol. Palaeoecol. 212, 119–140.

Gébelin, A., Mulch, A., Teyssier, C., Jessup, M.J., Law, R.D., Brunel, M., 2013. The Miocene elevation of Mount Everest. Geology 41, 799–802.

Harris, N., 2006. The elevation history of the Tibetan Plateau and its implications for the Asian monsoon. Palaeogeogr. Palaeoclimatol. Palaeoecol. 241, 4–15.

He, H.Y., Sun, J.M., Li, Q.L., Zhu, R.X., 2012. New age determination of the Cenozoic Lunpola Basin, central Tibet. Geol. Mag. 149, 141–145.

Hoorn, C., Ohja, T., Quade, J., 2000. Palynological evidence for vegetation development and climatic change in the sub-Himalayan zone (Neogene, Central Nepal). Palaeogeogr. Palaeoclimatol. Palaeoecol. 163, 133–161.

Hou, J.Z., D'Andrea, W.J., Huang, Y.S., 2008. Can sedimentary leaf waxes record D/H ratios of continental precipitation? Field, model, and experimental assessments. Geochim. Cosmochim. Acta 72, 3503–3517.

Jia, G.D., Wei, K., Chen, F.J., Peng, P.A., 2008. Soil *n*-alkane δD vs. altitude gradients along Mount Gonga, China. Geochim. Cosmochim. Acta 72, 5165–5174.

Jia, G.D., Li, Z.Y., Peng, P.A., Zhou, L.P., 2012. Aeolian *n*-alkane isotopic evidence from North Pacific for a Late Miocene decline of C_4 plant in the arid Asian interior. Earth Planet. Sci. Lett. 321/322, 32–40.

Kelly, C.K., Woodward, F.I., 1995. Ecological correlates of carbon isotope composition of leaves: a comparative analysis testing for the effects of temperature, CO_2 and O_2 partial pressures and taxonomic relatedness on $\delta^{13}C$. J. Ecol. 83, 509–515.

Kohn, F.J., 2010. Carbon isotope compositions of terrestrial C_3 plants as indicators of (paleo)ecology and (paleo)climate. Proc. Natl. Acad. Sci. U. S. A. 107, 19691–19695.

Körner, C., Farquhar, G.D., Roksandic, Z., 1988. A global survey of carbon isotope discrimination in plants from high altitude. Oecologia 74, 623–632.

Körner, C., Farquhar, G.D., Wong, S.C., 1991. Carbon isotope discrimination by plants follows latitudinal and altitudinal trends. Oecologia 88, 30–40.

Leier, A., Quade, J., DeCelles, P., Kapp, P., 2009. Stable isotopic results from paleosol carbonate in south Asia: paleoenvironmental reconstructions and selective alteration. Earth Planet. Sci. Lett. 279, 242–254.

Li, M.C., Liu, H.Y., Li, L.X., Yi, X.F., Zhu, X.J., 2007. Carbon isotope composition of plants along altitudinal gradient and its relationship to environmental factors on the Qinghai-Tibet Plateau. Pol. J. Ecol. 55, 67–78.

Li, J.Z., Wang, G.A., Liu, X.Z., Han, J.M., Liu, M., Liu, X.J., 2009. Variations in carbon isotope ratios of C_3 plants and distribution of C_4 plants along an altitudinal transect on the eastern slope of Mount Gongga. Sci. China Ser. D Earth Sci. 52, 1714–1723.

Liu, J., Yu, X.H., Yang, J.H., Liu, M.S., 2001. Geothermal history simulation in Lunpola Basin (Tibet). J. Jianghan Pet. Inst. 23, 19–21 (In Chinese).

Liu, W.G., Yang, H., Li, L., 2006. Hydrogen isotopic compositions of *n*-alkanes from terrestrial plants correlate with their ecological life forms. Oecologia 150, 330–338.

Luo, P., Peng, P.A., Gleixner, G., Zheng, Z., Pang, Z., Ding, Z., 2011. Empirical relationship between leaf wax *n*-alkane δD and altitude in the Wuyi, Shennongjia and Tianshan Mountains, China: implications for paleoaltimetry. Earth Planet. Sci. Lett. 301, 285–296.

Ma, P.F., Wang, L.C., Ran, B., 2013. Subsidence analysis of the Cenozoic Lunpola basin, central Qinghai-Tibetan Plateau. Acta Petrol. Sin. 29, 990–1002.

Magill, C.R., Ashley, G.M., Freeman, K.H., 2013. Water, plants, and early human habitats in eastern Africa. Proc. Natl. Acad. Sci. U. S. A. 110, 1175–1180.

Métais, G., Antoine, P.-O., Baqri, S.R.H., Crochet, J.-Y., Franceschi, D., Marivaux, L., Welcomme, J.-L., 2009. Lithofacies, depositional environments, regional biostratigraphy and age of the Chitarwata Formation in the Bugti Hills, Balochistan, Pakistan. J. Asian Earth Sci. 34, 154–167.

Molnar, P., Houseman, G.A., England, P.C., 2006. Palaeo-altimetry of Tibet. Nature 444, E4-E4.

Mora, C.I., Sheldon, B.T., Elliot, W.C., Driese, S.G., 1998. An oxygen isotope study of illite and calcite in three Appalachian Paleozoic vertic paleosols. J. Sediment. Res. 68 (3), 456–464.

Pedentchouk, N., Freeman, K.H., Harris, N.B., 2006. Different response of δD values of *n*-alkanes, isoprenoids and kerogen during thermal maturation. Geochim. Cosmochim. Acta 70, 2063–2072.

Polissar, P.J., Freeman, K.H., 2010. Effects of aridity and vegetation on plant-wax δD in modern lake sediments. Geochim. Cosmochim. Acta 74, 5785–5797.

Polissar, P.J., Freeman, K.H., Rowley, D.B., McInerney, F.A., Currie, B., 2009. Paleoaltimetry of the Tibetan Plateau from D/H ratios of lipid biomarkers. Earth Planet. Sci. Lett. 287, 64–76.

Quade, J., Cerling, T.E., 1995. Stable isotopes in paleosols and the expansion of C4 grasses in the late Miocene of Northern Pakistan. Palaeogeogr. Palaeoclimatol. Palaeoecol. 115, 91–116.

Quade, J., Breeckerm, D.O., Daëronm, M., Eilerm, J., 2011. The paleoaltimetry of Tibet: an isotopic perspective. Am. J. Sci. 311, 77–115.

Rao, Z.G., Jia, G.D., Zhu, Z.Y., Wu, Y., Zhang, J.W., 2008. Comparison of the carbon isotope composition of total organic carbon and long-chain n-alkanes from surface soils in eastern China and their significance. Chin. Sci. Bull. 53, 3921–3927.

Raymo, M.E., Ruddiman, W.F.e., 1992. Tectonic forcing of Late Cenozoic climate. Nature 359, 117–122.

Rowley, D.B., 2007. Stable isotope-based paleoaltimetry: theory and validation. Rev. Mineral. Geochem. 66, 23–52.

Rowley, D.B., Currie, B.S., 2006. Palaeo-altimetry of the late Eocene to Miocene Lunpola basin, central Tibet. Nature 439, 677–681.

Rowley, D.B., Garzione, C.N., 2007. Stable isotope-based paleoaltimetry. Annu. Rev. Earth Planet. Sci. 35, 463–508.

Sachse, D., Radke, J., Gleixner, G., 2004. Hydrogen isotope ratios of recent lacustrine sedimentary n-alkanes record modern climate variability. Geochim. Cosmochim. Acta 68, 4877–4889.

Sachse, D., Billault, I., Bowen, G.J., Chikaraishi, Y., Dawson, T.E., Feakins, S.J., Freeman, K.H., Magill, C.R., McInerney, F.A., van der Meer, M.T.J., Polissar, P., Robins, R.J., Sachs, J.P., Schmidt, H.-L., Sessions, A.L., White, J.W.C., West, J.B., Kahmen, A., 2012. Molecular paleohydrology: interpreting the hydrogen-isotopic composition of lipid biomarkers from photosynthesizing organisms. Ann. Rev. Earth Planet. Sci. 40, 221–249.

Saito, K., Yasunari, T., Takata, K., 2006. Relative roles of large-scale orography and land surface processes in the global hydroclimate. Part II: impacts on hydroclimate over Eurasia. J. Hydrometeorol. 7, 642–659.

Sessions, A.L., Burgoyne, T.W., Schimmelmann, A., Hayes, J.M., 1999. Fractionation of hydrogen isotopes in lipid biosynthesis. Org. Geochem. 30, 1193–1200.

Smith, F.A., Freeman, K.H., 2006. Influence of physiology and climate on δD of leaf wax n-alkanes from C3 and C4 grasses. Geochim. Cosmochim. Acta 70, 1172–1187.

Song, X.Y., Spicer, R.A., Yang, J., Yao, Y.F., Li, C.S., 2010. Pollen evidence for an Eocene to Miocene elevation of central southern Tibet predating the rise of the High Himalaya. Palaeogeogr. Palaeoclimatol. Palaeoecol. 297, 159–168.

Spicer, R.A., Harris, N.B.W., Widdowson, M., Herman, A.B., Guo, S.X., Valdes, P.J., Wolfe, J.A., Kelley, S.P., 2003. Constant elevation of southern Tibet over the past 15 million years. Nature 421, 622–624.

Sun, J.M., Xu, Q.H., Liu, W.M., Zhang, Z.Q., Xue, L., Zhao, P., 2014. Palynological evidence for the latest Oligocene–early Miocene paleoelevation estimate in the Lunpola Basin, central Tibet. Palaeogeogr. Palaeoclimatol. Palaeoecol. 399, 21–30.

Tian, L., Masson-Delmotte, V., Stievenard, M., Yao, T., Jouzel, J., 2001. Tibetan Plateau summer monsoon northward extent revealed by measurements of water stable isotopes. J. Geophys. Res. 106, 28081–28088.

Tipple, B.J., Pagani, M., 2007. The early origins of terrestrial C4 photosynthesis. Annu. Rev. Earth Planet. Sci. 35, 435–461.

Tipple, B.J., Meyers, S.R., Pagani, M., 2010. Carbon isotope ratio of Cenozoic CO2: a comparative evaluation of available geochemical proxies. Paleoceanography 25, PA3202. http://dx.doi.org/10.1029/2009PA001851.

Vogts, A., Moossen, H., Rommerskirchen, F., Rullkötter, J.R., 2009. Distribution patterns and stable carbon isotopic composition of alkanes and alkan-1-ols from plant waxes of African rain forest and savanna C3 species. Org. Geochem. 40, 1037–1054.

Wei, K., Jia, G., 2009. Soil n-alkane δ^{13}C along a mountain slope as an integrator of altitude effect on plant species δ^{13}C. Geophys. Res. Lett. 36, L11401. http://dx.doi.org/10.1029/2009GL038294.

Xu, Q., Ding, L., Zhang, L.Y., Cai, F.L., Lai, Q.Z., Yang, D., Jing, L.-Z., 2013. Paleogene high elevations in the Qiangtang Terrane, central Tibetan Plateau. Earth Planet. Sci. Lett. 362, 31–42.

Yuan, C.P., Xu, S.H., 2000. Characteristics of geotemperature field and maturity of source rocks in Lunpola basin, Xizang (Tibet). Exp. Petrol. Geol. 22 (2), 156–160 (In Chinese with English abstract).